FACILE SYNTHESIS OF DENSELY PACKED POLYHEDRAL Co$_3$V$_2$O$_8$ SUBMICRON PARTICLES WITH HIGH REVERSIBLE LITHIUM STORAGE CAPABILITY

L. LIU[*], W. ZHAO, Q. LIU, L. CHEN

Automotive Engineering Research Institute, Jiangsu University, Zhenjiang 212013, China

Polyhedral Co$_3$V$_2$O$_8$ submicron particles were successfully prepared by hydrothermal method followed by annealing, and employed as anode materials for lithium ion batteries. The polyhedral Co$_3$V$_2$O$_8$ submicron particles have smooth surface and are densely packed, which have advantages for maintaining structural integrity and accommodating the volume variation under repeated discharge-charge processes. Electrochemical measurement results showed that the as-prepared Co$_3$V$_2$O$_8$ delivered high reversible capacity and good rate capability, indicating a promising anode candidate for high performance lithium ion batteries.

1. Introduction

Lithium ion batteries (LIBs) have attracted great interest to meet the requirements of power sources for hybrid electric vehicles (HEVs) or electric vehicles (EVs). The energy density and power density of LIBs are highly dependent on the physical and chemical properties of both cathode and anode materials[1]. For anodes, the commercially used graphite carbon materials have almost reached the low theoretical capacity, which are insufficient to satisfy the market requirements[2]. Numerous efforts have been devoted to developing novel materials with high specific capacities, such as silicon[3], tin[4] etc. However, the rapid capacity decay resulting from large volume change via continuous lithiation-delithiation processes remains tremendous challenge for these semimetal/metal elements.

Recently, transition metal oxides have been studied and regarded as promising anode material candidates, due to their interfacial and synergistic effects of the multiple cation species[5]. As important mixed-metal oxides, metal vanadates including CuV$_2$O$_6$[6], MnV$_2$O$_6$[7], ZnV$_2$O$_6$[8] and Ag$_2$V$_4$O$_{11}$[9] etc., have been widely studied. Especially, cobalt vanadates (Co$_3$V$_2$O$_8$; CVO) were studied as anode for LIBs with excellent performance. Wang et al. firstly reported the Co$_3$V$_2$O$_8$ multilayered nanosheets as a novel anode for LIBs and explained the reversible conversion reactions between Co species proceeding on the amorphous Li$_x$V$_2$O$_5$ matrices[10]. A new phased Co$_3$V$_2$O$_8$·nH$_2$O hollow hexagonal prismatic pencils were synthesized and exhibited impressive lithium storage properties with excellent cycling stability, and rate capability[11]. Mai group used a facile one-pot method to obtain macroporous CoV$_2$O$_6$ nanosheets via acetylene black induced heterogeneous growth, which showed typical features of pseudocapacitive behavior[12]. Despite the progress in recent years, their practical applications are limited by capacity fading and low volumetric capacity, which greatly limits their industrial application[13]. By careful designing/controlling of the morphology and particle sizes, the dense structure, large particle size,

---

[*] Corresponding authors: lliu@ ujs.edu.cn

low specific surface area would dramatically reduce irreversible surface chemical reactions and improve the electrochemical stability[14].

In this work, polyhedral $Co_3V_2O_8$ submicron particles (denoted as P-CVO) were synthesized through hydrothermal method followed by annealing. Physical characterizations were carried out to examine the morphology and the crystalline structure. Electrochemical properties were investigated as anodes in P-CVO/Li half-cell and exhibit high electrochemical performance, which indicated a promising anode candidate for LIBs.

2. Experimental section

2.1. Synthesis section

All the chemicals are analytical grade and used without any further purification. Briefly, 1.0 mmol of ammonium metavanadate (NH_4VO_3) was firstly dissolved into 40 ml distilled water. Then, 1.5 mmol of cobalt nitrate hexahydrate ($Co(NO_3)_2 \cdot 6H_2O$) and 15 mmol of urea ($CO(NH_2)_2$) were slowly added to the above solution under stirring. The mixed solution were then transferred into a 50 ml Teflon-lined stainless autoclave and maintained at 180 ^{o}C for 12 h. After the autoclave was cooled down to room temperature, the precipitates were washed with distilled water and absolute ethanol for several times. Finally, the obtained precipitates were calcinated at 400 ^{o}C with a heating rate of 2 ^{o}C/min and maintained at the temperature for 4 h.

2.2. Sample Characterization

The crystalline structure of the samples are characterized by X-ray powder diffraction (XRD) with a Japan Rigaku D/max rA X-ray diffractometer equipped with graphite monochromatized high-intensity Cu-Kα radiation (λ = 1.54178 Å). The transmission electron microscopy (TEM) images are performed with a Hitachi Model H-800 instrument with a tungsten filament, using an accelerating voltage of 200 kV. High-resolution transmission electron microscopy (HRTEM) images and electron diffraction (ED) patterns are carried out on a JEOL-2010 TEM at an acceleration voltage of 200 KV. The field emission scanning electron microscopy (FE-SEM) images are taken on a FEI Sirion-200 SEM.

2.3. Electrochemical measurement

The working electrodes are prepared by mixing the as-prepared $Co_3V_2O_8$ samples, acetylene black and PTFE in a weight ratio of 70:20:10, with ethanol as a dispersant. The paste is then compressed into a thin piece with a roller and cut into a film disk of 8 mm in diameter. The film disks are dried at 80 °C for 12 h in vacuum oven for further use. Half-cells are assembled in an Ar-filled glove box. The lithium metal is used as counter electrode and reference electrode, and microporous Celgard-2300 is used as a separator. The electrolyte is comprised by 1.0 M lithium hexafluorophosphate ($LiPF_6$) dissolving into the mixed solvents of ethylene carbonate (EC)/dimethyl carbonate (DMC)/ethylene methyl carbonate (EMC) (v/v/v= 1:1:1). The galvanostatic discharge-charge tests are carried out in the potential range from 0.01 V to 3.0 V at ambient temperature, using the LAND-CT2001A instrument (Wuhan Jinnuo, China). The cyclic voltammetry (CV) measurements and impedance spectra are conducted with the Zahner Zennium E electrochemical workstation.

3. Results and discussion

The crystal structure of the as-prepared P-CVO is determined by X-ray diffraction (XRD) (Fig. 1a). All the peaks of P-CVO can be indexed to the orthorhombic phase (JCPDS No. 74-1487). The morphology and the microstructure are further studied by scanning electron microscopy (SEM) and transmission electron microscopy (TEM). A low-magnification SEM image (Fig 1b) panoramically indicates that P-CVO is consisted of well-crystallized nano or submicron particles with the particle size about 100-350 nm. It can be observed from the enlarged SEM in Fig 1c that the particles are densely stacked plane by plane and exhibit polyhedral shape with smooth surface. TEM images (Fig 1d) further confirmed that P-CVO is composed of several polyhedral-stacked

units through face to face to form a 3D dense structure. The high resolution TEM (HRTEM) image taken from the edge of the particle (Fig. 1d insert) clearly illustrates the legible ordered lattice fringes with basal spacing of 0.471 nm, which is consistent with the (120) lattice plane of orthorhombic $Co_3V_2O_8$. It is thought that such structure could increase tap density, which is originated from the dense structure of polyhedral closely stacking and the relatively large primary particle size[14]. Furthermore, the densely packed particles could also decrease specific surface, which could inhibit irreversible surface chemical reactions between electrode and electrolyte in discharge-charge processes.
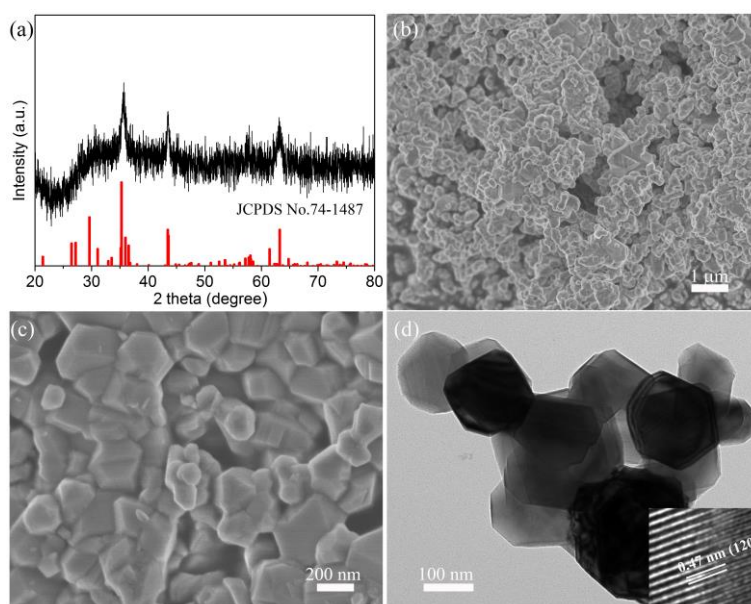
Fig. 1. (a) XRD patterns, (b) low-magnification SEM image, (c) high-magnification SEM image, and (d) TEM image (inset: corresponding HRTEM image) of the as-prepared P-CVO.
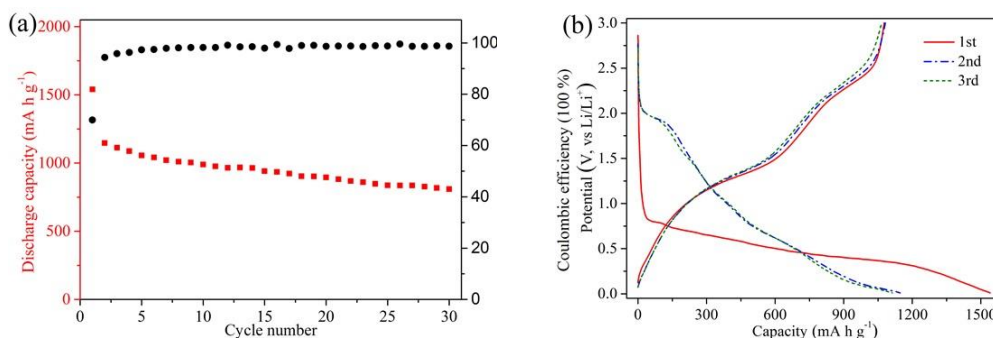
Fig. 2 (a) Cycling performance, (b) charge and discharge profiles at the current density of 100 mA g^{-1}.

The cycling performance of P-CVO electrode is evaluated by galvanostatic discharge-charge measurement at the current density of 100 mA g^{-1} in the voltage range of 0.01 V to 3.0 V (Fig 2a). The first discharge and charge capacity of P-CVO electrode is 1540 and 1077 mA h g^{-1}, respectively, corresponding to the Coulombic efficiency (CE) of 69.9 %. In the second cycle, the discharge capacity endured a fast capacity degradation and decreased to 1147 mA h g^{-1}. The sudden specific capacity decrease phenomenon is commonly observed for transition metal-oxides-based anode electrodes, which attributed to the presence of a possible activation

process in the electrode[15]. Then the reversible capacities become stable. After 30 cycles, the discharge capacity of P-CVO electrode can still be maintained at 809 mA h g^{-1}, with a corresponding CE greater than 98%.

The corresponding voltage capacity profiles are shown in Fig. 2b. In the first discharge curve, the potential drops quickly to 0.82 V. Then a plateau is shown and the capacity drops gradually. In the first charge curve, the plateaus at 2.8 and 2.4 V are due to the intercalation of Li$^+$ ions. This process is usually ascribed to irreversible reactions, i.e., formation of a solid electrolyte interphase (SEI) layer and defined as interfacial lithium storage. However, in the second discharge curve, two new plateaus are observed at 1.9 V and 0.6 V, which indicate that the anode is stable and shows the typical plateaus corresponding to the phase transitions of crystalline $Co_3V_2O_8$. The 3rd cycles shows no apparent differences compared to the 2nd cycle, indicating the excellent reversibility.
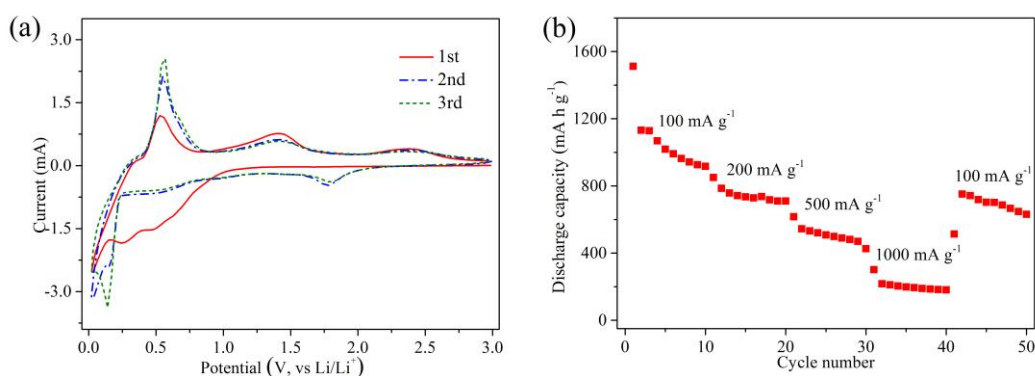
Fig. 3 (a) The cyclic voltammetries of the initial three cycles, (b) rate performance of the P-CVO at various current densities from 100 mA g^{-1} to 1000 mA g^{-1}.

To evaluate the electrochemical reversibility, the initial three curves of CV at a scan rate of 0.1 mV/s is presented in Fig. 3a. In the first cathodic sweep, two reduction peaks are observed: the peak at 0.47 might be associated with the reduction of $Co_3V_2O_8$ to CoO accompanied by the formation of $Li_xV_2O_5$; the reactions at around 0.25 V correspond to the further reduction into metallic Co and further lithiation of $Li_xV_2O_5$ to and the formation SEI. In the anodic sweep, three distinguished oxidation peaks centered at 0.53, 1.41 and 2.39 V are observed. These three peaks are assigned to the extraction of Li ions from $Li_{x+y}V_2O_5$ as well as $Li_xV_2O_5$ matrices, and the oxidation of metallic Co to CoO[10]. In the second cathodic sweep, a new peak is observed at 1.77 V, which can be attributed to the insertion of Li ions into the $Li_xV_2O_5$ matrix ($Li_xV_2O_5 + yLi \rightarrow Li_{x+y}V_2O_5$)[15]. The other two existing peaks have notable shifting compared to the first cycle (0.47 to 0.51 V; 0.25 to 0.12 V). The second anodic sweep exhibit similar three oxidation peaks and retained on subsequent cycling. All the peaks in the third cycle exhibit similar positions and indicate the structural integrity of the material.

The rate capability of the P-CVO electrodes is measured at different current density ranging from 100, 200, 500 and 1000 mA g^{-1}. In Fig. 3b, decrease in capacity with increasing discharge current can be clearly observed. At 100 mA g^{-1}, the average discharge capacity is 1060 mA h g^{-1}. Further increasing the current density, the values measured at every 10th cycle are further reduced to 747 mA h g^{-1} at 200 mA g^{-1}; 509 mA h g^{-1} at 500 mA g^{-1}. Even at 1000 mA g^{-1}, the discharge capacity retention can still up to 207 mA h g^{-1}. For the cycle completion back to 100 mA g^{-1}, the average specific capacity was up to 676 mA h g^{-1}.

4. Conclusions

In summary, the densely packed polyhedron $Co_3V_2O_8$ submicron particles are successfully prepared by a facile hydrothermal method followed by annealing. The P-CVO with grain size, high crystallinity and specific polyhedron nanostructures were used as anode materials for LIBs, which exhibit high specific capacity, great cycling stability and rate performance. The demands for higher chemical stability, lower cost, and easy synthesis make P-CVO as an attractive candidate to meet the increasing demand for high power LIBs.

Acknowledgements

References

[1] M. V. Reddy, G. V. Subba Rao, B. V. Chowdari, Chemical reviews **113**, 5364 (2013).
[2] W. J. Zhang, Journal of Power Sources **196**, 13 (2011).
[3] H. Wu, G. Yu, L. Pan, et al. Nature communications **4**, 1943 (2013).
[4] W. M. Zhang, J. S. Hu, Y. G. Guo, et al. Advanced Materials **20**, 1160 (2008).
[5] C. Yuan, H. B. Wu, Y. Xie, et al. Angewandte Chemie International Edition, **53**, 1488 (2014).
[6] W. Hu, X. Du, Y. Wu, et al. Journal of Power Sources **237**, 112 (2013).
[7] S. Zhang, R. Hu, L. Liu, et al. Materials Letters **124**, 57 (2014).
[8] F. K. Butt, F. Idrees, M. Tahir, et al. Materials Letters **155**, 15 (2015).
[9] P. J. Sideris, R. Yew, I. Nieves, et al. Journal of Power Sources **254**, 293 (2014).
[10] G. Z. Yang, H. Cui, G. W. Yang, et al. Acs Nano **8**, 4474 (2014).
[11] F. Wu, S. Xiong, Y. Qian, et al. Angewandte Chemie International Edition **54**, 10787 (2015).
[12] L. Zhang, K. Zhao, Y. Luo, et al. ACS Applied Materials & Interfaces **8**, 7139 (2016).
[13] L. S. Zhong, J. S. Hu, A. M. Cao, et al. Chemistry of Materials **19**, 1648 (2007).
[14] J. C. Fang, Y. F. Xu, G. L. Xu, et al. Journal of Power Sources **304**, 15 (2016).
[15] V. Soundharrajan, B. Sambandam, J. Song, et al. ACS Applied Materials & Interfaces **8**, 8546 (2016).